NANO LETTERS

2009
Vol. 9, No. 10
3435-3439

Piezoelectric Potential Gated Field-Effect Transistor Based on a Free-Standing ZnO Wire

Peng Fei,[†,‡,§] Ping-Hung Yeh,[†,‡] Jun Zhou,[‡] Sheng Xu,[‡] Yifan Gao,[‡] Jinhui Song,[‡] Yudong Gu,[‡,§] Yanyi Huang,[§] and Zhong Lin Wang*[,‡]

School of Materials Science and Engineering, Georgia Institute of Technology, Atlanta, Georgia 30332, and Department of Advanced Materials and Nanotechnology, College of Engineering, Peking University, 100084 Beijing, China

Received May 21, 2009; Revised Manuscript Received August 15, 2009

ABSTRACT

We report an external force triggered field-effect transistor based on a free-standing piezoelectric fine wire (PFW). The device consists of an Ag source electrode and an Au drain electrode at two ends of a ZnO PFW, which were separated by an insulating polydimethylsiloxane (PDMS) thin layer. The working principle of the sensor is proposed based on the piezoelectric potential gating effect. Once subjected to a mechanical impact, the bent ZnO PFW cantilever creates a piezoelectric potential distribution across it width at its root and simultaneously produces a local reverse depletion layer with much higher donor concentration than normal, which can dramatically change the current flowing from the source electrode to drain electrode when the device is under a fixed voltage bias. Due to the free-standing structure of the sensor device, it has a prompt response time less than 20 ms and quite high and stable sensitivity of 2%/μN. The effect from contact resistance has been ruled out.

One-dimensional (1D) nanomaterials have profound applications in biological and chemical sensing,[1,2] mechanical force and mass sensing,[3−5] nanoelectromechanics,[6] optoelectronics,[7] and electronics and photonics.[8−12] Nanodevices made using individual semiconductor nanowires/nanotubes/nanobelts are mostly laterally bonded on a flat substrate following the configuration of a field effect transistor (FET), in which the substrate serves as a gate electrode; the current transported from the drain to source along the nanowire is controlled or tuned by the applied gate voltage or the chemical/biochemical species adsorbed on the surface of the nanowires. Recently, using the coupled semiconductive and piezoelectric properties of ZnO, a group of nanodevices have been demonstrated utilizing the piezotronics effect,[13−16] the working principle of which relies on the piezoelectric potential created inside a nanowire under straining, which can serve as the gate voltage for fabricating a new type of FETs and diodes. In this paper, we demonstrate the first piezoelectric FET made using a free-standing ZnO wire for sensing transverse force/vibration. The working mechanism of the device depends on the piezoelectric field create at the root of the wire adjacent to the substrate, and it is distinct from traditional nanoforce/mass sensors that rely on the detection of oscillation frequency.[17−19] The free-standing piezoelectric FET has potential applications like hearing aids, atomic force microscopy (AFM) cantilevers, and security triggers.[20−22]

Most of the current nanodevices using 1D nanomaterials are usually bonded at the two ends, so that the two ends may not have the freedom to move. This type of configuration is not advantageous for fabricating devices that simulate the action of hairy beams inside an ear, possibly preventing them from measuring nanoscale air or liquid flow. To overcome this difficulty, we aim at proposing a free-standing piezoelectric FET (FS PE-FET) based on the piezotronic effect. This device was first proposed based on numerical simulation about the distribution of a piezoelectric potential in a ZnO wire when it is subjected to mechanical straining.[23] For a vertical free-standing ZnO wire, once it is bent by an external force that is uniformly applied perpendicular to the wire along its length, a piezoelectric potential drop is created across the wire. On the basis of a static model calculation with considering the screening effect of free charge carriers, for a vertical ZnO wire on an identical ZnO substrate with a donor concentration $p = 1 \times 10^{23}/m^3$, diameter $d = 25$ nm, and length $l = 600$ nm, when a total external force of $f_y = 800$ nN was uniformly applied normal to the wire at its side surface, the piezoelectric potential distribution across the bent wire oriented with its c-axis

* Corresponding author, zlwang@gatech.edu.
† These authors contributed equally to this work.
‡ Georgia Institute of Technology.
§ Peking University.

10.1021/nl901606b CCC: $40.75
Published on Web 09/09/2009

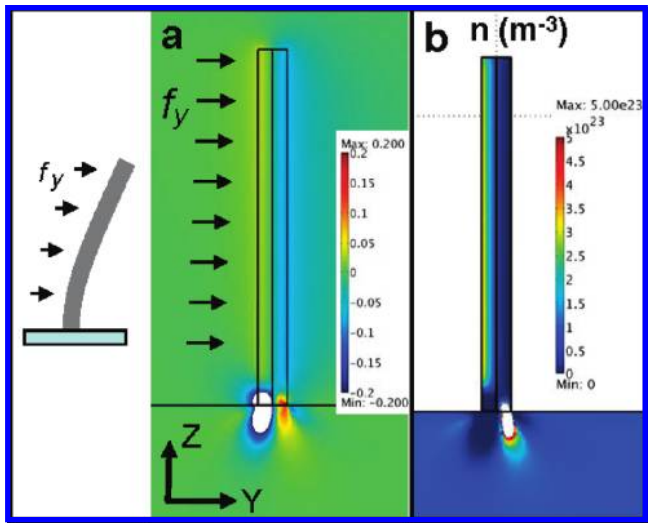

Figure 1. Theoretical modeling of piezoelectric potential distribution and donor concentration distribution in a bent free-standing ZnO wire. (a) Plot of piezoelectric potential distribution φ for a donor concentration $n = 1 \times 10^{23}/m^3$ after considering screening effect by free charge carriers using a static model. A schematic diagram of the vertical wire is shown at the left. The dimension of the wire is width $d = 25$ nm, length $l = 600$ nm There is a potential region at the junction of the ZnO wire and ZnO substrate, which shows a reverse potential distribution comparing to the upper part of the wire with positive potential at the compressive side and negative potential at the tensile side. The blank region is the region where $\varphi \ll -0.2$ V. (b) Corresponding donor concentration distribution in the bent nanowire. Due to the piezoelectric potential, across the width of junction region, a depletion layer with lower donor concentration and a reverse depletion layer with higher donor concentration are generated at the compressive and tensile sides. The blank region is the region where the donor concentration is so high in the range of $n \gg 5 \times 10^{23}/m^3$. It should be noted that, for simplicity, the calculation was carried out for a ZnO nanowire that is epitaxially grown on a ZnO substrate. The actual distribution of piezoelectric potential could be different from that shown in (a), but the qualitative characteristics such as the reverse potential region should still exist.

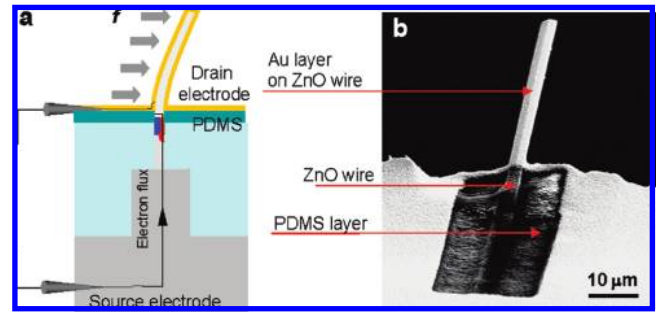

Figure 2. Design of the device. (a) Design of a free-standing ZnO PFW cantilever sensor device. In this device, a free-standing cantilever makes it easily to response to a tiny external force and then show a piezoelectric effect. At the same time, in its working status, the free charge carriers are guaranteed to flow through the junction region between the cantilever part and on-substrate part to make sure the force-induced variation of electrical property can be detected by the measurement system. (b) SEM image of a device after side-cutting using a FIB for showing the inner structure of the fabricated device.

pointing upward at room temperature (RT) is shown in Figure 1a, which displays the contour plot of the piezoelectric potential inside and around the wire. An outstanding feature noticed in Figure 1a is that there is a reverse potential distribution at the junction region between the wire and the substrate, with the compressive strained region positive and the tensile strained region negative. The significant large magnitude of this transverse potential forces the n-type charge carriers (electrons) to accumulate at the compressive region to partially screen the local positive piezoelectric potential, resulting in highly concentrated electron carriers at the region near the root (Figure 1b). At the same time, when the conduction band is pushed down by the piezoelectric polarization on the compression side, the electrons will be strongly degenerate with a very high density. Therefore, the increase of free electron density is much larger than the decrease on the tensile side. Consequently, the TOTAL number of free charge carriers near the wire root would increase. The overall effect is thus an increase in the conductance. This expected result is different from the behavior of the two-ends contacted piezoelectric FET.[4] The existence of this local "necking region" with superhigh carrier density is the core of our device presented below.

To utilize the piezoelectric potential created at the root region, a new type of FS-FET has been built, as shown in Figure 2a, in which ZnO is partially embedded in a substrate and partially standing out. After coating the top part with metal and bottom part near the root with a protective insulating PDMS layer, we applied a bias from the bottom of the wire and the metal contact using two probes. The insulative layer at the root region can effectively minimize the equal potential effect introduced by the metal layer coated at the top part and thus protects the bottom reverse depletion region. Thus a FS PE-FET is configurated, in which the channel formed by the piezopotential at the wire−substrate junction forces the electrons to flow through the region where there are accumulated charge carriers (e.g., the positive piezoelectric potential region). Since the magnitude of the piezopotential increases almost linearly with the applied force or degree of wire bending, the transported current is a measure of the force. This is the principle of the piezoelectric potential gated transistor, which is a sensor for measuring the transversely applied force on the wire.

The FS PE-FET was fabricated by using thin film deposition techniques and manipulation under an optical microscope (Figure S1 in Supporting Information). Figure 2a is a schematic diagram of the designed structure. A scanning electron microscope (SEM) image taken from a device after side cutting using a focused ion beam (FIB) microscope shows the inner structure of the device (Figure 2b). The Au−PDMS−ZnO layered structure is clear from the image. It also makes sure that the key functioning parts of the ZnO wire and the Ag source electrode are not shorted by Au deposition. For the electrical measurement of this sensor device, two tungsten tips were contacted, respectively, with the Ag source electrode and Au drain electrode for connecting the device to the measurement system, Keithley 4200. After we applied a bias voltage $V = (V_s - V_d)$ between the source and drain electrodes, the free charge carriers will flow through the rooted region of the ZnO PFW where a

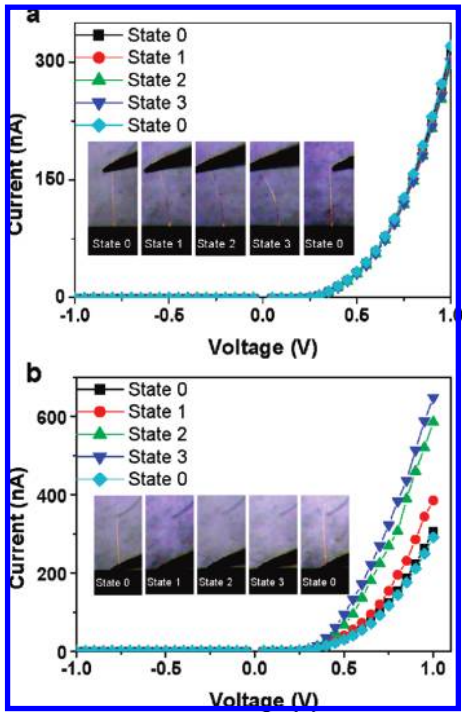

Figure 3. Experiment performed for proving the necessity of the junction piezoelectric potential in the device. (a) The top of ZnO cantilever was pushed and then released by an insulator tip four times, and the corresponding $I-V$ curves were measured. The $I-V$ curves did not change in a total of five status checks. Inserted are the optical images of the corresponding five status checks. (b) The bottom of the ZnO cantilever was also pushed and then released four times. The $I-V$ curves changed between every two status checks. The conductivity of the device became better and better when it was bent step by step and then gradually recovered to the original status when it was released step by step.

high profile of local accumulated free charge carriers exist (Figure 2a). From the $I-V$ curve we measured (Figure 3a), there is a Schottky barrier between the source electrode and ZnO PFW. When the PFW is transversely bent by an external force, a piezoelectric potential is created across the root junction region adjacent to the substrate, which may play a similar role as the gate voltage applied between the gate and the base electrode in a MOS FET device. So, this is considered as a kind of piezoelectric potential gated FET.[2]

Proving the reverse piezoelectric potential distribution across the junction region is a key point to the device; the top of ZnO cantilever was transversely pushed and released step by step for a total of four times using an aluminum oxide coated insulator tip, which was mounted on a high-resolution positioner (Figure 3a). The $I-V$ curve showed no response to the PFW deformation, possibly because the tip touched the PFW at its tip so that the strain field created at the root was not strong enough to drive the FET. Then we change the pushing position of the PFW to close to its root (Figure 3b). In this case, the degree of local deformation was large enough, so that the $I-V$ curve showed sensitive change. With the increase of the degree of bending, the increase in conductance is obvious. After retracting the tip and setting the PFW to free, the $I-V$ curve recovered to its original shape. This set of experiments shows that the piezoelectric potential created at the root of the PFW is effective for tuning the transported electrical current and it can be used as a force sensor.

To reveal the relationship between the deformation and the electrical variation, the PFW was bent step by step and then released step by step. Under a constant bias voltage of $V = 0.5$ V, the corresponding change in current is plotted in Figure 4a, which shows four steps up and four steps down. Such an experiment was repeated four times, and a good reproducibility was received. By defining the current measured at strain free status as I_0, the relative variation in current is plotted as a function of wire transverse deflection at tip (Figure 4b). A linear relationship was received, and the curves for applying the stress and releasing the stress overlap very well.

To quantify the electrical signal in responding to mechanical deformation provided by the tip, we calibrated the mechanical characteristics of the PFW using AFM. The AFM tip pushed the PFW from the side with its tip in contact mode; the mechanical property of the PFW was determined from the force−displacement curve. The local contact configuration of the AFM tip with the PFW was determined from the vertical displacement of the tip (Figure S2a in Supporting Information), and the mechanical behavior was characterized by the transverse deflection distance of the tip (Figure S2b in Supporting Information). The contact point of the tip with the PFW was chosen to be the point at which the probe was applied as in Figure 4a. The transverse force was plotted as a function of the displacement of the AFM tip (Figure S2c in Supporting Information). The curve is approximately linear at small displacement, and it can be characterized by a slope of $K_{f\text{-}d} \sim 2\ \mu N/\mu m$ (Figure 4c). Combining Figure 4b and Figure 4c, a quantitative relationship is established between the transverse force that the AFM tip applied to the AFM cantilever (external stimulation) with the current variation rate of the device (inner response), which are plotted in Figure 4d. The curve is approximately linear with a slope of $s_{v\text{-}f} \sim 2\%\ /\mu N$, which strongly indicates a fairly stable relationship between the stimulation force and the device response.

The sensor device could also be activated by a gas flow. When an argon gas flow pulse was transversely applied to a ZnO cantilever with a 5 s cycle, the cantilever was impacted and bent with a corresponding periodic current peak measured under a fixed bias of 0.5 V (Figure 5a). The highest current peak detected here was 180 nA; in comparison with the baseline of 120 nA, the corresponding variation rate is 50%. One peak was extracted for showing detailed profile (inset in Figure 5a). It has a risetime of ~20 ms, which indicates the response speed of the device is faster than 20 ms with considering the electronic response of the measurement system. Periodic continuous gas blowing was also applied to the ZnO cantilever with a 5 s cycle. The corresponding current output is shown in Figure 4b. All of the observed results are entirely consistent to the principle proposed for the device and show its sensitivity. The stability of the device has also been examined (Figure S3 in Supporting Information).

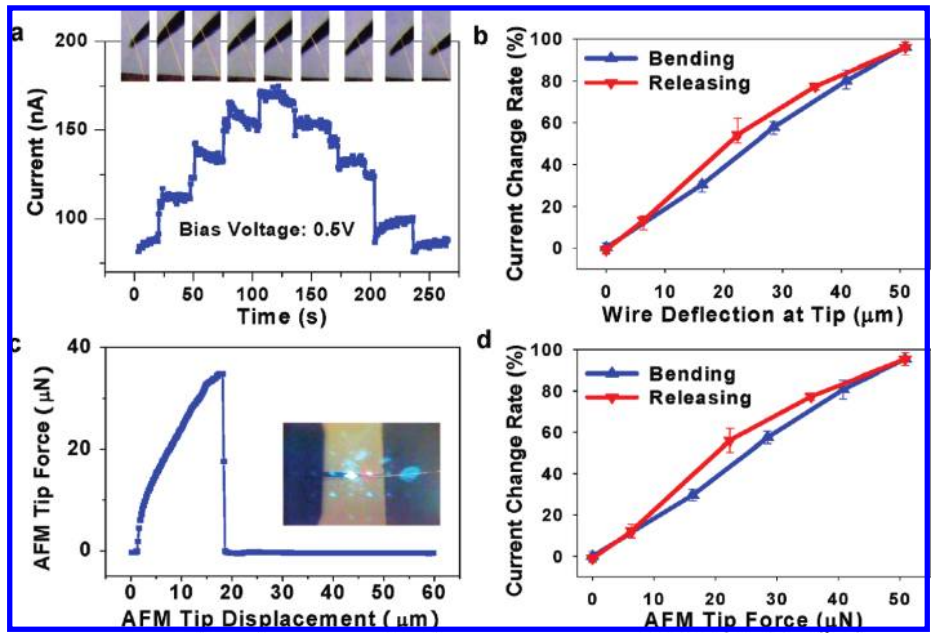

Figure 4. Quantifying the relationship between the force applied and the corresponding electrical response of a FS-FET. (a) The cantilever was bent step by step for four times and then released step by step for four times at the middle region. Current outputs were measured under a fixed bias of 0.5 V. Inserted are the corresponding optical images of the PFW for the nine cantilever bending statuses. (b) Measured relationship between the current variation rate and the transverse deflection of the PFW. The current variation is defined as $\Delta = (I_i - I_0)/I_0$, where I_0 is the current measured under strain free status of the cantilever, and I_i is current under strain. (c) AFM calibration of the mechanical behavior of the PFW in order to determine the relationship between its transverse deflection of the externally applied force (see Figure S2 in Supporting Information for details). (d) Calibrated relationship between the force applied to the PFW and the corresponding measured electrical current for the FS-FET at a fixed bias of 0.5 V.

The working principle of the device has been suggested due to the piezoelectric potential at the root of the wire. What are the other factors that may contribute to the observed effect? One effect could be contact resistance, but this factor has been ruled out based on following experiments. First, if the contact resistance were the dominant contribution, the resistance would be expected to be increased once the device is mechanically triggered by an external force due to the "losing contact" effect, which is in contrast to our observation shown in Figure 4. Second, the high repeatability of the performance received from 20 devices in our study suggests that contact resistance cannot explain the phenomenon we have observed. Finally, we have designed an alternative experiment to rule out the effect from contact resistance. We used a Kevlar fiber as the core wire, on which a polycrystalline ZnO layer of thickness 500 nm was coated around the fiber by sputtering. Then, the fiber was used to fabricate the device following the same procedure as described in Figure S1 in Supporting Information. The electrical measurement from two devices showed no change in conductance by deforming the wire using a insulative probe (Figure S4 in Supporting Information). This is because the coating layer composed of randomly oriented polycrystalline ZnO nanocrystals shows no macroscopic piezoelectric effect. As concluded from the above discussions and additional experiments, we believe that contact resistance is not the cause of the effect reported in Figures 3−5.

In summary, we have demonstrated a piezoelectric potential gated and external force triggered FET using a free-standing ZnO piezoelectric fine wire (PFW). In this device,

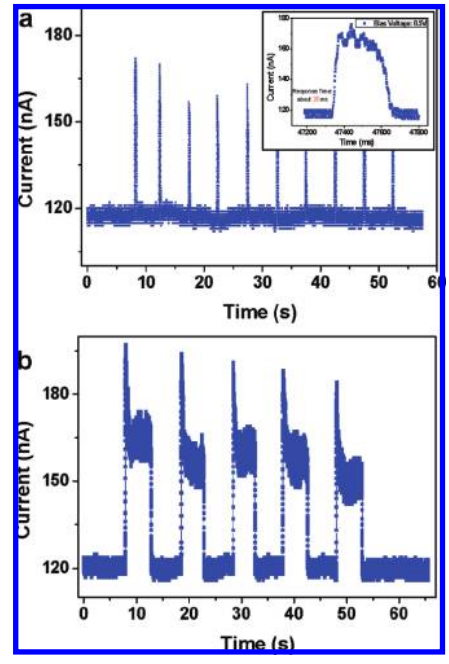

Figure 5. Response of a FS-FET to periodic gas blowing for demonstrating its potential application for measuring the transverse force/pressure. (a) The current transported by the FS-FET at a fixed bias of 0.5 V when argon gas was blown at the PFW as short pulses. The inset is a detailed shape of the current signal, showing a response time of ~20 ms even without deconvoluting the electronic response time of the measurement system. (b) The current transported by the FS-FET at a fixed bias of 0.5 V when argon gas was blown periodically for 5 s each cycle.

the key functional part is the junction region at the root of the ZnO PFW, which is buried inside the PDMS layer. The working principle of the device is suggested as follows. Once subjected to mechanical impact, the bent ZnO PFW cantilever creates a piezoelectric potential distribution across its width in this junction region and simultaneously produces local depletion and reverse depletion layers, which triggers and controls the device. The size of the area and the local donor concentration of the reverse depletion layer are both dominated by the external force/pressure/vibration induced piezoelectric potential. The sensor device has been proved to have a high piezoelectric potential control sensitivity (~micronewtons) in micrometer scale due to the free-standing cantilever structure and fairly stable linear relationship between the mechanical stimulation and its electrical response. At the same time, it has a response time less than 20 ms. The FS-FET device demonstrated here could have potential applications as hearing aids, AFM cantilevers, force/pressure sensors, and security systems.

Methods. ***Synthesis of Long ZnO Wires.*** The long ZnO wires were grown using a vapor−solid process.[24] ZnO powder was used as the source material and loaded in an alumina boat located at the center of an alumina tube (75 cm), which was placed in a single-zone horizontal tube furnace. Argon gas was used as carrier gas at a flow rate of 50 standard cubic centimeters per minute (sccm) throughout the experiment. An alumina substrate with length of 10 cm was loaded 20 cm downstream from the source material. The furnace was heated to 1475 °C and was held at that temperature for 4.5 h under a pressure of ~250 mbar. Then the furnace was turned off, and the tube was cooled down to room temperature under an argon flow.

Device Fabrication. The FS PE-FET was fabricated by the following procedures. First, single crystal long ZnO piezoelectric fine wires (PFWs) were used in our experiment, which were ~400 μm in length ~4 μm in diameter and were synthesized by thermal evaporation.[14] The large size PFWs were chosen for easy manipulation under an optical microscope. The sample principle applies to smaller nanowires. Second, a glass slice with typical length of ~2 cm, width of ~1 cm, and thickness of ~1.5 mm was prepared. The slice was washed with deionized water and ethanol. After drying with flowing nitrogen gas and baking in a furnace at 80 °C for 15 min, the glass slice was ready to be used as an insulating substrate. Third, the ZnO PFW was placed on the glass substrate with part of the wire standing out of the edge and forming a cantilever structure. Silver paste was applied to affix the end of ZnO wire on the substrate and form the source electrode (Figure S1a.1 in Supporting Information). Fourth, a thin layer of polydimethylsiloxane (PDMS) was used to package part of the Ag electrode and the on-substrate part of the wire. The thickness of this PDMS layer is larger than the diameter of the wire and the thickness of the silver electrode to make sure the wire and the electrode were insulated inside the PDMS. By this important step, the source electrode can avoid short-circuiting with the Au drain electrode that is to be deposited in the next step and the preservation of the piezoelectric potential generated at the junction region by minimizing the equipotential effect introduced by Au deposition. After being baked at 80 °C for 30 min, the PDMS layer was fully polymerized and functioned well as an insulating layer (Figure S1a.2 in Supporting Information). Lastly, the device was shadowed by a mask so that an Au film was deposited only at the top free-standing segment by E-beam evaporator (Figure S1a.3 and Figure S1a.4 in Supporting Information). As the triggering part of the sensor device, the cantilever was a core−shell Au−ZnO structure with the Au shell working as drain electrode of the device (Figure S1a.5 in Supporting Information). SEM images of the fabricated FS PE-FET are shown in Figure 1d.

Acknowledgment. This research was supported by DARPA, BES DOE, and NSF. P.F. and Y.D.G. are grateful for the fellowship support by the China Scholarship Council (CSC) (No. 20073020). We acknowledge the kind help from Chi-Te Huang for using the FIB.

Supporting Information Available: Figures showing the fabrication process of the FS-FET, a quantitive experiment using AFM to reveal the relationship between applied mechanical force and measured electrical response, the stability of a typical device, and an alternative experiment to rule of the effect from contact resistance. This material is available free of charge via the Internet at http://pubs.acs.org.

References

(1) Cui, Y.; Wei, Q.; Park, H.; Lieber, C. M. *Science* **2001**, *293*, 1289.
(2) Patolsky, F.; Timko, B. P.; Yu, G.; Fang, Y.; Greytak, A. B.; Zheng, G.; Lieber, C. M. *Science* **2006**, *313*, 1100.
(3) Jensen, K.; Kim, K.; Zettl, A. *Nat. Nanotechnol.* **2008**, *3* (9), 533.
(4) Wang, X. D.; Zhou, J.; Song, J. H.; Liu, J.; Xu, N. S.; Wang, Z. L. *Nano Lett.* **2006**, *6*, 2768.
(5) Zhou, J.; Fei, P.; Gao, Y. F.; Gu, Y. D.; Liu, J.; Bao, G.; Wang, Z. L. *Nano Lett.* **2008**, *8* (9), 2725.
(6) Sazonova, V.; Yaish, Y.; Ustunel, H.; Roundy, D.; Arias, T. A.; McEuen, P. L. *Nature* **2004**, *431*, 284.
(7) Duan, X. F.; Huang, Y.; Agarwal, R.; Lieber, C. M. *Nature* **2003**, *421*, 241.
(8) Tans, S. J.; Verschueren, A. R. M.; Dekker, C. *Nature* **1998**, *393*, 49.
(9) Bachtold, A.; Hadley, P.; Nakanishi, T.; Dekker, C. *Science* **2001**, *294*, 1317.
(10) Javey, A.; Guo, J.; Wang, Q.; Lundstrom, M.; Dai, H. J. *Nature* **2003**, *424*, 654.
(11) Huang, M.; Mao, S.; Feick, H.; Yan, H.; Wu, Y.; Kind, H.; Weber, E.; Russo, R.; Yang, P. D. *Science* **2001**, *292*, 1897.
(12) Fasth, C.; Fuhrer, A.; Samuelson, L.; Golovach, V. N.; Loss, D. *Phys. Rev. Lett.* **2007**, *98*, 266801.
(13) Zhou, J.; Gu, Y. D.; Fei, P.; Mai, W. J.; Gao, Y. F.; Yang, R. S.; Bao, G.; Wang, Z. L. *Nano Lett.* **2008**, *8* (9), 3035.
(14) Zhou, J.; Fei, P.; Gu, Y. D.; Mai, W. J.; Gao, Y. F.; Yang, R. S.; Bao, G.; Wang, Z. L. *Nano Lett.* **2008**, *11* (8), 3973.
(15) Wang, Z. L. *Adv. Funct. Mater.* **2008**, *18*, 3553.
(16) Wang, Z. L. *Adv. Mater.* **2007**, *19*, 889.
(17) Mamin, H. J.; Rugar, D. *Appl. Phys. Lett.* **2001**, *79*, 3358.
(18) Ekinci, K. L.; Huang, X. M. H.; Roukes, M. L. *Appl. Phys. Lett.* **2004**, *84*, 4469.
(19) Poncharal, P.; Wang, Z. L.; Ugarte, D.; De Heer, W. A. *Science* **1999**, *283*, 1513.
(20) Wu, G. H.; Datar, R. H.; Hansen, K. M.; Thundat, T.; Cote, R. J.; Majumdar, A. *Nat. Biotechnol.* **2001**, *19*, 856.
(21) Chen, G. Y.; Thundat, T.; Wachter, E. A.; Warmack, R. J. *J. Appl. Phys.* **1995**, *77*, 3618.
(22) Shekhawat, G.; Tark, S. H.; Dravid, V. P. *Science* **2006**, *311*, 1592.
(23) Gao, Y. F.; Wang, Z. L. *Nano Lett.* **2009**, *9* (3), 1103.
(24) Pan, Z. W.; Dai, Z. R.; Wang, Z. L. *Science* **2001**, *291*, 1947.

NL901606B